

Self-Templating of Metal-Driven Supramolecular Self-Assembly: A General Approach toward 1D Inorganic Nanotubes

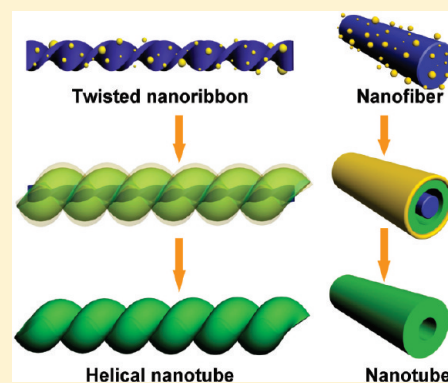
Yan Qiao, Yijie Wang, Zhiyi Yang, Yiyang Lin, and Jianbin Huang*

Beijing National Laboratory for Molecular Sciences (BNLMS), State Key Laboratory for Structural Chemistry of Unstable and Stable Species, College of Chemistry and Molecular Engineering, Peking University, Beijing 100871, P.R. China

S Supporting Information

ABSTRACT: The rational design of one-dimensional (1D) inorganic nanomaterials directed by self-assembled soft matters is one of the most attractive subjects in modern chemistry. In this work, the self-templating approach based on metal–cholate supramolecular self-assemblies is reported, which is distinct from the traditional soft template method. Under the framework of *self-templating*, metal ions can serve as both the inorganic precursor and constituent of the template; additional precursors which may change the solution conditions and interfere with the soft templates are not needed. It is demonstrated that self-templating method is a general approach to synthesize a series of 1D inorganic nanotubes including ZnS, CuS, NiS, CdS, CoS, ZnSe, and ZnTe nanotubes. Moreover, the structural diversity and dynamic nature of organic architectures allow the preparation of size and shape-adjustable 1D nanotubes through conveniently temporal and thermal controls. A possible mechanism for nanotube formation is also proposed.

KEYWORDS: nanomaterials, self-assembly and self-assembled materials, semiconductors



INTRODUCTION

In nature, many examples exist of inorganic nanostructures with well-defined architectures and functions.¹ The diverse morphologies and exquisite organization can be modulated by organic proteins and polysaccharides with complicated patterns of various functional groups.² Inspired by Nature, self-assembled soft matters with structural diversity and dynamic nature have been utilized as templates to mediate the mineralization of inorganic species, giving birth to sophisticated architectures.³ One of the interesting topics in soft template approach lies in the transcriptions of soft template structures into the resultant nanomaterials. In particular, the traditional soft template protocol has been successfully exploited to synthesize silica nanomaterials with controllable size, shape, helicity, and porosities.⁴ However, semiconductor and metal nanomaterials with retained morphologies are less reported.⁵ Two issues exist concerning this problem. In some cases, soft templates may lose their structural characteristics in the presence of inorganic precursors. This is because precursors (often metal ions) can change the solution conditions, for example, ionic strength, and interfere with the self-assembled structures. In other cases, the interaction between soft templates and precursors is often too weak to ensure the morphological replica from organic templates to inorganic species. It is therefore of significance to develop a reliable method to transcribe the self-assembled nanostructures into semiconductor and metal nanomaterials.

One-dimensional (1D) inorganic materials, especially nanotubes, are of immense scientific and technological interest owing

to the beneficial influence of dimensionality on electronic and optical materials.⁶ Important examples are carbon and kinds of semiconductor nanotubes. During last few decades the majority of work has been reported to explore new routes to synthesize inorganic nanotubes, such as decomposition of the precursor, vapor deposition, solvothermal, vapor–liquid–solid, and hard template method.⁷ These methods, although they succeed in generating some specific nanomaterials, are usually incapable of becoming a general route to create a series of inorganic nanotubes. Besides, the preparation conditions of these approaches are often tough.

In our previous work, self-assembled 1D nanostructures are reported in the system of sodium cholate (SC) and a series of metal ions.⁸ On the basis of these metal-driven self-assemblies, the *self-templating approach* is developed in this paper to synthesize 1D inorganic nanotubes. Under the framework of *self-templating approach*, metal ions can serve as both the inorganic precursor and constituent of the soft template, which are further deposited from supramolecular self-assemblies and generate inorganic nanomaterials with corresponding shape. Additional precursors which may change the solution conditions and interfere with the soft templates are not needed. Particularly, the metal–ligand cooperation between metal precursor and organic template is strong enough to ensure successful structural transcription from soft template into inorganic species. The self-templating approach

Received: September 15, 2010

Revised: December 6, 2010

Published: February 01, 2011

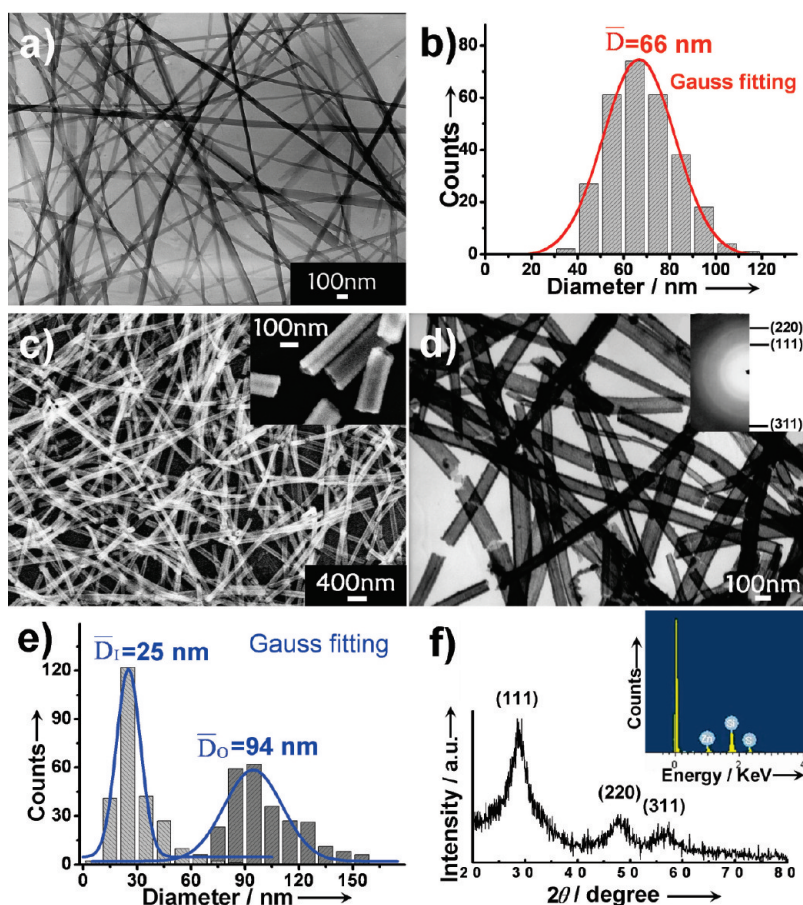


Figure 1. Zinc-cholate supramolecular nanofibers at 25 °C: (a) TEM image; (b) histogram of diameter distribution. ZnS nanotubes prepared at 25 °C: (c) FE-SEM; (d) TEM image and ED pattern (inset); (e) histogram of the inner and outer diameter distribution; (f) XRD and EDS data (inset). Herein, \bar{D}_i is the nanofiber diameter and \bar{D}_i and \bar{D}_O are the inner and outer diameters of the ZnS nanotube, respectively.

offers such advantages as (1) it is a general method to prepare a series of inorganic materials such as metal sulfides, metal selenides, and metal telluride; (2) inorganic nanotubes are conveniently obtained by adding depositing reagents into metal-cholate supramolecular self-assemblies under ambient conditions; (3) benefiting from the environmental responsiveness of soft template, the shape and size of as-synthesized inorganic materials could be readily controlled by adjusting the temporal and thermal conditions; (4) the approach is characterized by a one-step process, which can avoid post-processing procedures to remove the templates and give relatively pure products in comparison with the hard template route; and (5) inorganic nanotubes can be achieved in high yields.

EXPERIMENTAL SECTION

Materials. Sodium cholate (Alfa Aesar, 99%), metal nitrates, and other chemicals (A.R. Grade of Beijing Chemical Co.) were used as received.

Preparation of Metal-cholate Self-Assembled Nanofibers. The metal-cholate supramolecular systems were obtained by mixing sodium cholate solution with concentrated metal nitrates solution (0.1 or 0.5 M) followed by appropriate vortex and equilibration at desired temperature. During this period, a self-supporting and uniform hydrogel can be prepared. These samples were then applied to TEM and SEM, in which metal-cholate nanofiber can be observed.

Preparation of Metal Sulfide Nanotubes. In a typical synthesis, 2 mL of metal-cholate supramolecular hydrogel (for example, 5 mM/5 mM for zinc-cholate, copper-cholate, and cadmium-cholate, or 20 mM/20 mM for nickel-cholate and cobalt-cholate) was added with 1 N 100 mM Na_2S solution (for ZnS, NiS, CdS, and CoS), 1 N 100 mM thioacetamide solution (for CuS), 1 N 100 mM sodium hydrogen selenide solution (for ZnSe), and 1 N 100 mM sodium hydrogen telluride solution (for ZnTe). For the preparation of ZnSe and ZnTe nanotubes, the solution should be kept under oxygen-free conditions. Agitation was not needed. The deposition reactions occurred at the interface of hydrogel and precipitator solution. After the reaction was completed, hydrogel was totally destroyed and the precipitate at the bottom of the test tube was collected by centrifugation and washed with deionized water several times.

Characterization of Supramolecular Nanofibers. A slice of hydrogel was placed on a copper grid or clean silicon sheet and then dried freely under ambient conditions and the desired temperature. Then the nanofibers were characterized by transmission electron microscopy (TEM, JEM-100CX, 100 kV) together with scanning electron microscopy (SEM, Hitachi S4800, 5 kV).

Characterization of Inorganic Nanomaterials. The obtained nanotubes were characterized by SEM (Hitachi S4800, 10 kV), TEM (JEOL JEM-200CX, 100 kV), HRTEM (FEI Tecnai F30, 300 kV), and XRD (Rigaku Dmax-2000, Ni-filtered $\text{Cu K}\alpha$ radiation). For the TEM and SEM measurements, the obtained products were dispersed in water and dropped onto a Formvar-covered copper grid and a silicon wafer, respectively, followed by drying naturally. For XRD measurements, several

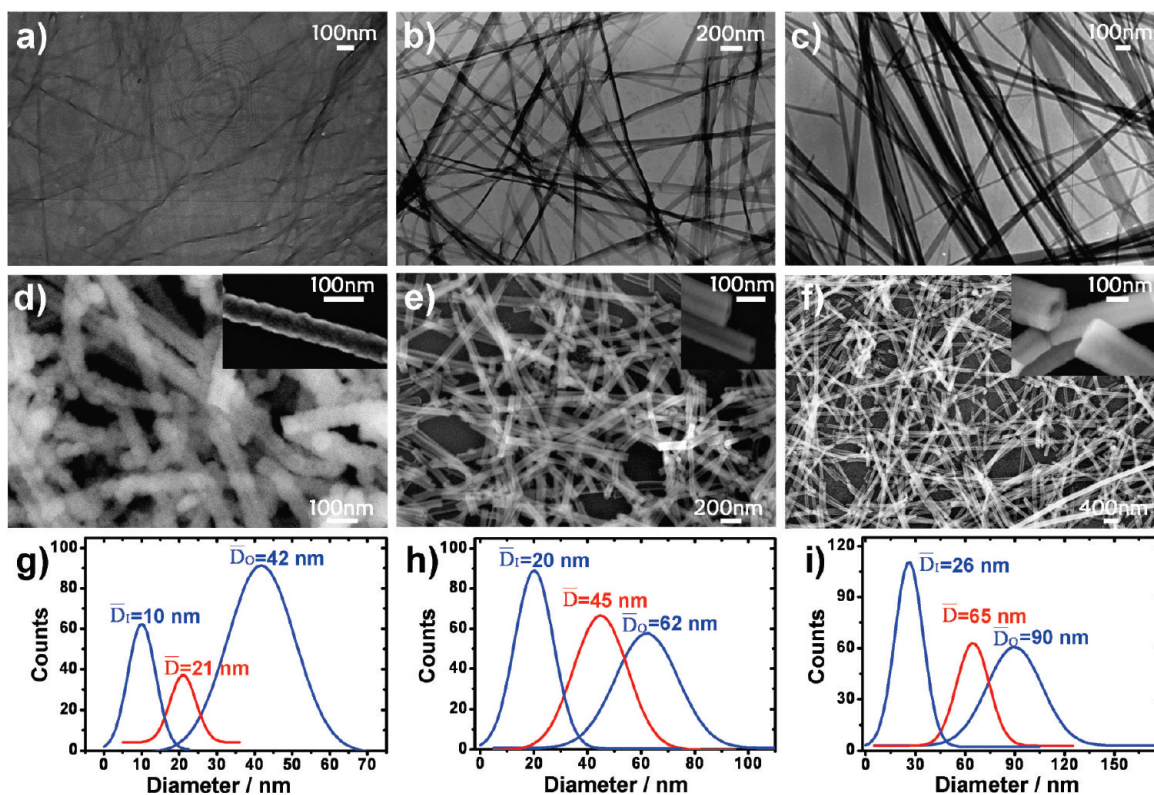


Figure 2. Zinc–cholate supramolecular nanofibers incubated at 20 °C for (a) 3 h; (b) 12 h; and (c) 24 h. As prepared ZnS nanotubes with different incubation times: (d) 3 h; (e) 12 h; (f) 24 h. The corresponding diameter statistics are shown in g–i.

drops of the suspension were dropped on a clean glass slide, followed by drying in the air.

RESULTS AND DISCUSSION

Preparation of ZnS Nanotubes Based on Zinc–Cholate Supramolecular Self-Assembly. As a representative demonstration, the preparation of ZnS nanotubes based on zinc–cholate supramolecular system will be discussed in detail. As shown in transmission electron microscopy (TEM, Figure 1a) and field emission scanning electron microscopy (FE-SEM, Supporting Information Figure S1), self-assembled nanofibers with lengths of micrometers are spontaneously formed in the zinc–cholate system at 25 °C. The statistical distribution of fiber diameters collected from TEM images shows the fiber diameters are in the range of 20–120 nm (Figure 1b). The mean diameter calculated by Gauss fitting is 66 nm. With the introduction of Na₂S solution, ZnS nanotubes can be deposited from zinc–cholate supramolecular nanofibers. SEM and TEM images (Figure 1c,d) provide large scale views of massive uniform ZnS nanotubes several micrometers long. The external and inner diameters of ZnS nanotubes are 25 and 94 nm, respectively, as calculated by Gauss fittings (Figure 1e). The inset SEM image in Figure 1c clearly exhibits the broken open end of nanotubes. The electron diffraction (ED) pattern (inset of Figure 1d) illustrates that the nanotubes are polycrystalline and adopt a cubic structure. The high-resolution TEM image (Supporting Information Figure S2) indicates the interplanar spacing of 0.31 nm, corresponding to the (111) planes of cubic ZnS. The atomic ratio of Zn to S in these nanotubes was determined by energy-dispersive spectroscopy (EDS) to be roughly 1:1 (inset of Figure 1f). X-ray diffraction (XRD) (Figure 1f)

shows the sphalerite structure (JCPDS no. 05-0566). It is also noted that the structural size and morphology of ZnS tubes are in good agreement with zinc–cholate nanofibers, which manifests the successful transcription of soft template into ZnS nanotubes.

ZnS Nanotubes with Tunable Size and Morphology.

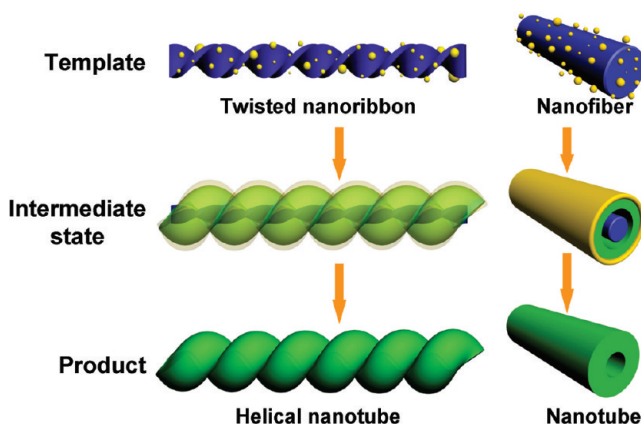
Moreover, the structural parameter of self-assembled zinc–cholate nanofibers can be tuned by varying temporal and thermal conditions. As Supporting Information Figure S3 shows, the self-assembled nanofiber diameter increases gradually with incubation time until reaching equilibration. The kinetics of nanofibers growth is greatly affected by environmental temperature: higher temperature will promote fiber growth and shorten the equilibration time. For instance, the equilibration time of zinc–cholate nanofiber (5 mM/5 mM) at 20, 25, and 60 °C is 24, 4, and 1 h. In spite of the difference in equilibration time, the equilibrated zinc–cholate nanofibers are of similar diameters at different equilibration temperatures. For example, the fibers equilibrated at 20, 25, and 60 °C will all have the diameters of 20–120 nm and mean diameter about 60–70 nm. Interestingly, zinc–cholate helical nanofibers are observed at 20 °C within three hours after sample preparation (Figure 2a). The nanohelices exhibit a twisted shape of nanoribbons with uniform bias and about 150 nm helical pitches, several nanometers thickness, and 10–30 nm in width. After nine hours, the nanohelices transform into nontwisted nanofibers (Figure 2b) with the diameters ranging from 20 to 80 nm. After 24 h of incubation, the system reaches equilibration (Figure 2c) and the fibers have a similar diameter to that in 25 °C. The corresponding histograms of diameter distribution are provided in Supporting Information Figure S4. The average fiber diameter analyzed by Gauss fitting increases from 21 and 45 to 65 nm when the sample is equilibrated at 20 °C for 3 h, 9 h, and 24 h (Figure 2g–i).

It is shown that zinc–cholate self-assembly undergoes structural evolution from twisted nanoribbons at the early stage to nontwisted nanofibers with increasing diameters as the incubation time extends ($T = 20\text{ }^{\circ}\text{C}$). This is because twisted nanoribbons are not stable structures which may require additional energy to compensate the bend energy. As the time proceeds, these twisted ribbons will transform into nontwisted nanofibers which are more stable. Another characteristic of this system is that higher temperature can promote fiber growth and shorten the equilibration time. The unique property of temperature effect is supposed to arise from hydroxyl groups of cholate molecules which may form hydrogen bonds with water and contribute to cholate hydrophilicity. When the temperature is raised, the hydrogen bonds between water and cholate hydroxyl groups are weakened, leading to higher hydrophobicity of zinc–cholate complex. As a consequence, the aggregating capability of zinc–cholate complex is promoted and fiber growth is accelerated.

Considering the tunability in shape, size, and helicity, these self-assembled fibers are supposed to be superior templates for synthesizing tunable nanomaterials by controlling thermal and temporal conditions. According to this idea, Na_2S solution is added to zinc–cholate samples at the incubation times of 3, 12, and 24 h at $20\text{ }^{\circ}\text{C}$, and ZnS nanotubes with adjustable shapes and diameters are prepared (Figure 2d–f). In the zinc–cholate system with 3 h of incubation time, helical ZnS nanotubes are obtained. SEM (Figure 2d) and TEM (Supporting Information Figure S5) images shows ZnS helical nanotubes with external diameters of 20–70 nm and inner diameters of 2–30 nm. The structural size and morphology of the ZnS helical nanotube is comparable to that of zinc–cholate helical fibers. An intimate investigation revealed that the diameter and helix pitches of helical nanotubes can be also varied (Supporting Information Figures S6 and S7). As the incubation time increases, diameter-tunable nanotubes without helicity are attained. In the zinc–cholate system with 12 h incubation, ZnS nanotubes with average external diameters of 62 nm and inner diameters 20 nm are obtained. When the incubation time of the zinc–cholate system was increased to 24 h, ZnS nanotubes with larger size were achieved. In all these cases, the diameters of zinc–cholate nanofibers are found to be greater than the inner diameters of ZnS nanotubes but smaller than their outer diameters.

Mechanism of the Self-Templating Method. As shown above, ZnS nanotubes with tunable sizes and morphology can be prepared through a self-templating method in zinc–cholate supramolecular systems. On the basis of the aforementioned results, the mechanism of ZnS nanotubes formation is outlined in Scheme 1, which involves three steps: (1) sulfide ions from Na_2S solution and metal ions in Zn–cholate hydrogel encounter on the surface of zinc–cholate nanofibers; (2) the wall of ZnS nanotube is built up on the reaction interface; (3) as the reaction proceeds, self-assembled nanofibers are consumed and inorganic nanotubes are consequently attained. A snapshot of the intermediate state of nanotube formation (Step 2) is presented in Supporting Information Figure S8 to demonstrate the connection between zinc–cholate nanofibers and as-prepared ZnS nanotubes. During the deposition process, the zinc–cholate supramolecular nanostructure acts as both zinc source and soft template for the subsequent preparation. It can be inferred from the proposed mechanism that the inorganic nanotubes will have smaller inner diameters and larger outer diameters compared with the size of the supramolecular nanofiber. Besides, the formation of ZnS nanotube is mainly attributed to the solubility difference between ZnS and zinc–cholate complex.

Scheme 1. Schematic Diagram of the Self-Templating Protocol



Benefiting from the diversity of available replacement reactions, this self-templating approach is expected to be extended for fabricating various 1D inorganic nanotubes.

Preparation of Metal Sulfide Nanotubes. A series of metal–cholate supramolecular nanofibers driven by Cu^{2+} , Ni^{2+} , Cd^{2+} , and Co^{2+} are observed (Figure 3a–d). The diameter distributions of nanofibers are shown in Supporting Information Figure S9a–d. On the basis of these metal-driven nanofibers, inorganic nanotubes of various metal sulfides are synthesized via the self-templating approach. SEM (Figure 3e–h) and TEM (Supporting Information Figure S10a–d) images indicate CuS, NiS, CdS, and CoS nanotubes are achieved in high yield and good uniformity. EDS microanalysis (Supporting Information Figure S10m–p) and powder XRD (Supporting Information Figure S10q–t) have proven the successful synthesis of covellite structured CuS (JCPDS no. 06-0464), NiAs-type NiS (JCPDS no. 77-1624), zinc blende structured CdS (JCPDS no. 10-0454), and jaipurite structured CoS (JCPDS no. 75-0605). ED patterns indicate that hexagonal phase CuS and NiS nanotubes are single crystal (Supporting Information Figure S10e,g) while face-centered cubic phase CdS and hexagonal phase CoS nanotubes are polycrystalline (Supporting Information Figure S10i,k). HR-TEM reveals that the tubes are highly crystallized and gives typical interplanar spacing (Supporting Information Figure S10f,h,j,l). For example, the HRTEM image of CuS nanotubes shows an interplanar spacing of 0.304 nm (Supporting Information Figure S10f), which corresponds to the (102) plane. It is noteworthy that the diameter of the soft template is bigger than the inner diameter of inorganic nanotubes while smaller than the outer one (Figure 4i–l).

It should be noticed that Na_2S is used as a sulfide source to prepare NiS, CdS, and CoS nanotubes while thioacetamide (TAA) is used for CuS nanotubes. When Na_2S solution is added to the copper–cholate sample, immediate precipitate without regular nanostructures will form. It is suggested that the choice of sulfide source is determined by the strength of metal–sulfide affinity which can be expressed by the solubility product constant. The solubility product constant of metal sulfide follows the sequence as $K_{\text{sp}}(\text{NiS}) (3.2 \times 10^{-19}) > K_{\text{sp}}(\text{CoS}) (4.0 \times 10^{-21}) > K_{\text{sp}}(\text{ZnS}) (1.6 \times 10^{-24}) > K_{\text{sp}}(\text{CdS}) (8.0 \times 10^{-27}) \gg K_{\text{sp}}(\text{CuS}) (6.3 \times 10^{-36})$.⁹ It can be noted that the $K_{\text{sp}}(\text{CuS})$ is greatly smaller than $K_{\text{sp}}(\text{NiS})$, $K_{\text{sp}}(\text{CdS})$, $K_{\text{sp}}(\text{CoS})$, and $K_{\text{sp}}(\text{ZnS})$; in other words, the deposition of CuS from supramolecular fibers is highly active. In the presence of Na_2S , the deposition of CuS is so fast that the

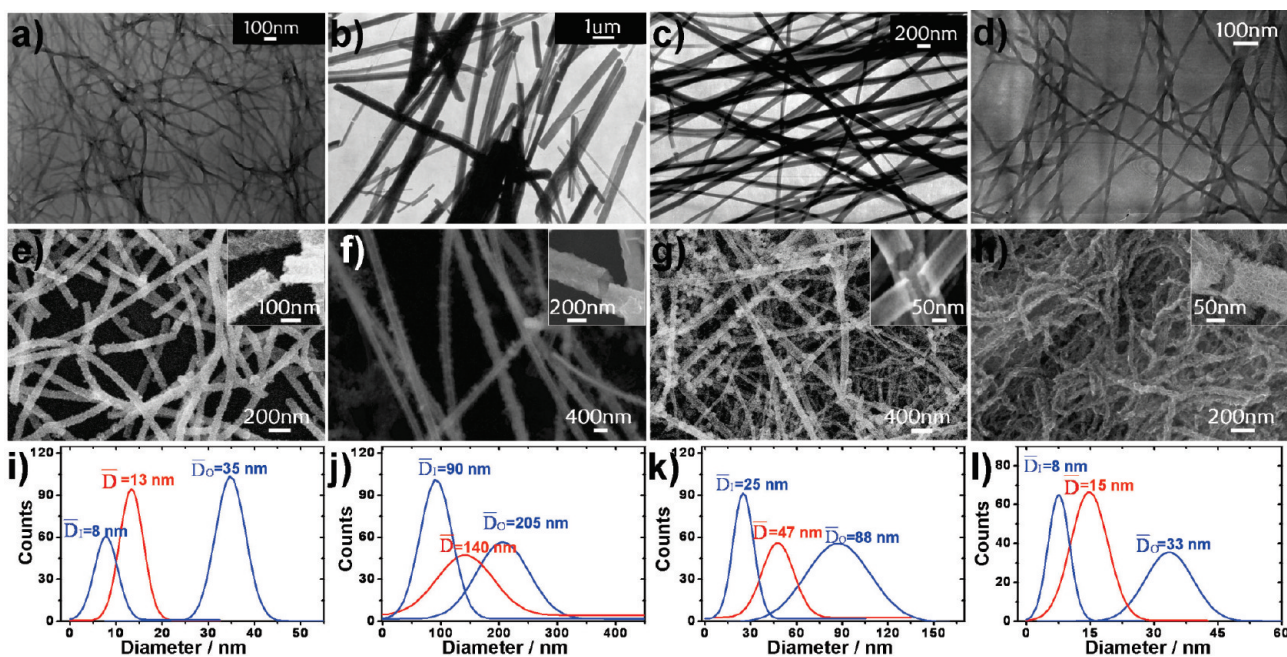


Figure 3. TEM images of nanofibers in the system of (a) Cu-cholate; (b) Ni-cholate; (c) Cd-cholate; and (d) Co-cholate at 25 °C. Metal sulfide nanotubes prepared from self-templating strategy: (e) CuS; (f) NiS; (g) CdS; and (h) CoS. The corresponding diameter statistics are shown in i–l.

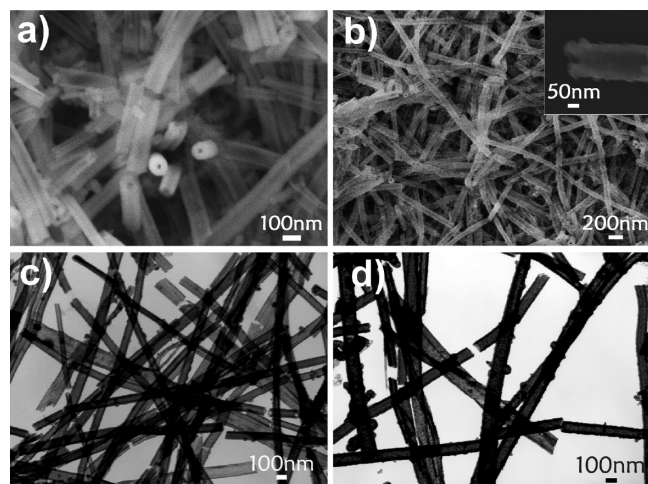


Figure 4. Zinc chalcogenides nanotubes prepared by self-templating strategy. SEM images (a, b) and TEM images (c, d) for ZnSe nanotubes (a, c) and ZnTe nanotubes (b, d).

controlled growth of nanomaterials induced by soft template is more difficult and irregular CuS precipitations are obtained. Compared with Na_2S , TAA is a gentle sulfide source that can generate CuS nanotubes in a more moderate speed. This rule of self-templating approach is instructive for choosing the reactant agent.

Preparation of Zinc Chalcogenide Nanotubes. One-dimensional nanotubes of metal selenides and metal tellurides could be also be produced through the self-templating approach following similar experimental procedures. For example, well-defined ZnSe and ZnTe nanotubes are readily synthesized from zinc-cholate supramolecular systems when NaHSe and NaHTe are used as depositing agents (Figure 4 and Supporting Information Figure S11). EDS microanalysis demonstrates that the atomic ratio of Zn/Se or Zn/Te in these nanotubes was roughly 1:1. The diameter of as-prepared

inorganic nanotubes is proven to be in agreement with self-assembled nanofibers.

CONCLUSIONS

In conclusion, we have developed a general self-templating approach to synthesize 1D inorganic nanotubes under mild conditions with a one-step process and massive products. The adjustable shape and size of supramolecular architectures allow the preparation of tunable 1D inorganic nanotubes by temporal and thermal controls. Benefiting from the diversity of available replacement reactions, this self-templating approach can be easily extended to create different kinds of 1D inorganic nanotubes. Moreover, it can be rationally envisioned that multiple compositional nanotubes may be constructed when multi-metal-ion assembly and/or multi-reactant-agent is employed in this synthetic strategy. This strategy is therefore believed to provide a simple and convenient route to create 1D inorganic nanomaterials with controllable shape, size, and helicity. We hope that this study may help provide understanding of nature's creation of the inorganic species in the process of biomineralization.

ASSOCIATED CONTENT

S Supporting Information. SEM study of zinc-cholate nanofiber; HRTEM image of ZnS nanotube; TEM images of the nanofibers with different incubation time; histograms of width distribution studies; helical zinc sulfide nanotubes; intermediate state of zinc sulfide nanotube formation; and characteristics of metal sulfides and ZnSe and ZnTe nanotubes (PDF). This material is available free of charge via the Internet at <http://pubs.acs.org>.

AUTHOR INFORMATION

Corresponding Author

*E-mail: jbhuang@pku.edu.cn. Fax: 86-10-62751708. Tel: 86-10-62753557.

ACKNOWLEDGMENT

This work was supported by National Natural Science Foundation of China (20873001, 20633010, 50821061, and 21073006) and National Basic Research Program of China (Grant No. 2007CB936201).

REFERENCES

- (1) (a) Aizenberg, J.; Weaver, J. C.; Thanawala, M. S.; Sundar, V. C.; Morse, D. E.; Fratzl, P. *Science* **2005**, *309*, 275. (b) Stanley, S. M. *Chem. Rev.* **2008**, *108*, 4483. (c) Hildebrand, M. *Chem. Rev.* **2008**, *108*, 4855. (d) Meldrum, F. C.; Cölfen, H. *Chem. Rev.* **2008**, *108*, 4332.
- (2) (a) Dicherson, M. B.; Sandhage, K. H.; Naik, R. R. *Chem. Rev.* **2008**, *108*, 4935. (b) Behrens, S. S. *J. Mater. Chem.* **2008**, *18*, 3788. (c) Bigall, N. C.; Reitzig, M.; Naumann, W.; Simon, P.; van Pée, K.-H.; Eychmüller, A. *Angew. Chem., Int. Ed.* **2008**, *47*, 7876. (d) Nam, K. T.; Kim, D. W.; Yoo, P. J.; Chiang, C. Y.; Meethong, N. L.; Hammond, P. T.; Chiang, Y. M.; Belcher, A. M. *Science* **2006**, *312*, 885. (e) Xie, J. P.; Zheng, Y. G.; Ying, J. Y. *J. Am. Chem. Soc.* **2009**, *131*, 888.
- (3) (a) Kijima, T.; Yoshimura, T.; Uota, M.; Ikeda, T.; Fujikawa, D.; Mouri, S.; Uoyama, S. *Angew. Chem., Int. Ed.* **2004**, *43*, 228. (b) Boettcher, S. W.; Fan, J.; Tsung, C. K.; Shi, Q. H.; Stucky, G. D. *Acc. Chem. Res.* **2007**, *40*, 784. (c) Wan, Y.; Zhao, D. Y. *Chem. Rev.* **2007**, *107*, 2821. (d) Colfen, H.; Mann, S. *Angew. Chem., Int. Ed.* **2003**, *42*, 2350. (e) Llusar, M.; Sanchez, C. *Chem. Mater.* **2008**, *20*, 782. (f) Lu, Y. F. *Angew. Chem., Int. Ed.* **2006**, *45*, 766. (g) van Bommel, K. J. C.; Friggeri, A.; Shinkai, S. *Angew. Chem., Int. Ed.* **2003**, *42*, 980.
- (4) (a) Pouget, E.; Dujardin, E.; Cavalier, A.; Moreac, A.; Valery, C.; Marchi-Artzner, V.; Weiss, T.; Renault, A.; Paternostre, M.; Artzner, F. *Nat. Mater.* **2007**, *6*, 434. (b) Yuan, Y. J.; Hentze, H. P.; Arnold, W. M.; Marlow, B. K.; Antonietti, M. *Nano Lett.* **2002**, *2*, 1359. (c) Seddon, A. M.; Patel, H. M.; Burkett, S. L.; Mann, S. *Angew. Chem., Int. Ed.* **2002**, *41*, 2988. (d) Kim, W. J.; Yang, S. M. *Chem. Mater.* **2000**, *12*, 3227. (e) Jung, J. H.; Ono, Y.; Hanabusa, K.; Shinkai, S. *J. Am. Chem. Soc.* **2000**, *122*, 5008. (f) Jung, J. H.; Shinkai, S.; Shimizu, T. *Chem. Mater.* **2003**, *15*, 2141. (g) Jung, J. H.; Kobayashi, H.; van Bommel, K. J. C.; Shinkai, S.; Shimizu, T. *Chem. Mater.* **2002**, *14*, 1445. (h) Delclos, T.; Aime, C.; Pouget, E.; Brizard, A.; Huc, L.; Delville, M.-H.; Oda, R. *Nano Lett.* **2008**, *8*, 1929. (i) Wu, X. W.; Jin, H. Y.; Liu, Z.; Ohsuna, T.; Terasaki, O.; Sakamoto, K.; Che, S. *Chem. Mater.* **2006**, *18*, 241. (j) Wan, Y.; Shi, Y. F.; Zhao, D. Y. *Chem. Commun.* **2007**, 897. (k) Caruso, R. A.; Antonietti, M. *Chem. Mater.* **2001**, *13*, 3272. (l) Caruso, R. A.; Antonietti, M. *Adv. Func. Mat.* **2002**, *12*, 307. (m) Lin, Y.; Qiao, Y.; Gao, C.; Tang, P. F.; Liu, Y.; Li, Z. B.; Yan, Y.; Huang, J. B. *Chem. Mater.* **2010**, *22*, 6711.
- (5) (a) Sone, E. D.; Zubarev, E. R.; Stupp, S. I. *Angew. Chem., Int. Ed.* **2002**, *41*, 1705. (b) Ma, N.; Dooley, C. J.; Kelley, S. O. *J. Am. Chem. Soc.* **2006**, *128*, 12598. (c) Kang, S. H.; Bozhilov, K. N.; Myung, N. V.; Mulchandani, A.; Chen, W. *Angew. Chem., Int. Ed.* **2008**, *47*, 5186. (d) Lee, S. W.; Mao, C. B.; Flynn, C. E.; Belcher, A. M. *Science* **2002**, *296*, 892.
- (6) (a) Rao, C. N. R.; Govindaraj, A. *Adv. Mater.* **2009**, *21*, 4208. (b) Bae, C.; Yoo, H.; Kim, S.; Lee, K.; Kim, J.; Sung, M. M.; Shin, H. *Chem. Mater.* **2008**, *20*, 756. (c) Chen, J. Y.; Wiley, B. J.; Xia, Y. N. *Langmuir* **2007**, *23*, 4120. (d) Kong, J.; Franklin, N. R.; Zhou, C. W.; Chaplin, M. G.; Peng, S.; Cho, K. J.; Dai, H. J. *Science* **2000**, *287*, 622. (e) Cademartiri, L.; Ozin, G. A. *Adv. Mater.* **2009**, *21*, 1013. (f) Xia, Y. N.; Yang, P. D.; Sun, Y. G.; Wu, Y. Y.; Mayers, B.; Gates, B.; Yin, Y. D.; Kim, F.; Yan, H. Q. *Adv. Mater.* **2003**, *15*, 353. (g) Carny, O.; Shalev, D. E.; Gazit, E. *Nano Lett.* **2006**, *6*, 1594.
- (7) (a) Nath, M.; Rao, C. N. R. *J. Am. Chem. Soc.* **2001**, *123*, 4841. (b) Chen, J.; Li, S. L.; Tao, Z. L.; Shen, Y. T.; Cui, C. X. *J. Am. Chem. Soc.* **2003**, *125*, 5284. (c) Tang, C. C.; Bando, Y.; Liu, B. D.; Golberg, D. *Adv. Mater.* **2005**, *17*, 3005. (d) Wang, X.; Zhuang, J.; Chen, J.; Zhou, K. B.; Li, Y. D. *Angew. Chem., Int. Ed.* **2004**, *43*, 2017. (e) Bakkers, E. P. A. M.; Verheijen, M. A. *J. Am. Chem. Soc.* **2003**, *125*, 3440.
- (8) (a) Qiao, Y.; Lin, Y. Y.; Wang, Y. J.; Liu, J.; Yang, Z. Y.; Yan, Y.; Huang, J. B. *Nano Lett.* **2009**, *9*, 4500. (b) Qiao, Y.; Lin, Y. Y.; Yang, Z. Y.;

Chen, H. F.; Zhang, S. F.; Yan, Y.; Huang, J. B. *J. Phys. Chem. B* **2010**, *114*, 11725.

(9) Dean, J. A. *Lange's Handbook of Chemistry*, 15th ed.; McGraw-Hill: New York, 1999; pp 1.331–1.342.